

Resolving R_D and R_{D^*} anomalies

Suman Kumbhakar, Ashutosh Kumar Alok, Dinesh Kumar and S Uma Sankar

Abstract The current world averages of the ratios $R_{D^{(*)}}$ are about 4σ away from their Standard Model prediction. These measurements indicate towards the violation of lepton flavor universality in $b \rightarrow c l \bar{\nu}$ decay. The different new physics operators, which can explain the $R_{D^{(*)}}$ measurements, have been identified previously. We show that a simultaneous measurement of the polarization fractions of τ and D^* and the angular asymmetries A_{FB} and A_{LT} in $B \rightarrow D^* \tau \bar{\nu}$ decay can distinguish all the new physics amplitudes and hence uniquely identify the Lorentz structure of new physics.

1 Introduction

In recent years, the evidence for charged lepton universality violation is observed in the charge current process $b \rightarrow c \tau \bar{\nu}$. The experiments, BaBar, Belle and LHCb, made several measurements of the ratios

$$R_D = \frac{\Gamma(B \rightarrow D \tau \bar{\nu})}{\Gamma(B \rightarrow D \{e/\mu\} \bar{\nu})}, \quad R_{D^*} = \frac{\Gamma(B \rightarrow D^* \tau \bar{\nu})}{\Gamma(B \rightarrow D^* \{e/\mu\} \bar{\nu})}. \quad (1)$$

Suman Kumbhakar
Indian Institute of Technology Bombay, Mumbai 400076, India, e-mail: suman@phy.iitb.ac.in

Ashutosh Kumar Alok
Indian Institute of Technology Jodhpur, Jodhpur 342011, India, e-mail: akalok@iitj.ac.in

Dinesh Kumar
University of Rajasthan, Jaipur 302004, India, e-mail: dinesh@uniraj.ac.in

S Uma Sankar
Indian Institute of Technology Bombay, Mumbai 400076, India, e-mail: uma@phy.iitb.ac.in

The current world averages of these measurements are about 4σ away from the Standard Model (SM) predictions [1].

All the meson decays in eq. (1) are driven by quark level transitions $b \rightarrow c\bar{l}\bar{\nu}$. These transitions occur at tree level in the SM. The discrepancy between the measured values of R_D and R_{D^*} and their respective SM predictions is an indication of presence of new physics (NP) in the $b \rightarrow c\tau\bar{\nu}$ transition. The possibility of NP in $b \rightarrow c\mu\bar{\nu}$ is excluded by other data [2]. All possible NP four-Fermi operators for $b \rightarrow c\tau\bar{\nu}$ transition are listed in ref. [3]. In ref [2], a fit was performed between all the $b \rightarrow c\tau\bar{\nu}$ data and each of the NP interaction term. The NP terms, which can account for the all $b \rightarrow c\tau\bar{\nu}$ data, are identified and their Wilson coefficients (WCs) are calculated. It was found that there are six allowed NP solutions. Among those six solutions, four solutions are distinct with a different Lorentz structure. In ref. [4] it was found that the tensor NP solution could be distinguished from other possibilities provided $\langle f_L \rangle$, the D^* polarization fraction can be measured with an absolute uncertainty of 0.1.

Here, we consider four angular observables, $P_\tau(D^*)$ (τ polarization fraction), f_L (D^* polarization fraction), A_{FB} (the forward-backward asymmetry), A_{LT} (longitudinal-transverse asymmetry) in the decay $B \rightarrow D^*\tau\bar{\nu}$. Note that these asymmetries can only be measured if the momentum of the τ lepton is reconstructed. We show that a measurement of these four quantities can uniquely identify the Lorentz structure of the NP operator responsible for the present discrepancy in R_D and R_{D^*} [5].

2 Distinguishing different new physics solutions

The most general effective Hamiltonian for $b \rightarrow c\tau\bar{\nu}$ transition can be written as

$$H_{eff} = \frac{4G_F}{\sqrt{2}}V_{cb} \left[O_{VL} + \frac{\sqrt{2}}{4G_F V_{cb}} \frac{1}{\Lambda^2} \left\{ \sum_i (C_i O_i + C'_i O'_i + C''_i O''_i) \right\} \right], \quad (2)$$

where G_F is the Fermi coupling constant, V_{cb} is the Cabibbo-Kobayashi-Maskawa (CKM) matrix element and the NP scale Λ is assumed to be 1 TeV. We also assume that neutrino is always left chiral. The effective Hamiltonian for the SM contains only the O_{VL} operator. The explicit forms of the four-fermion operators O_i , O'_i and O''_i are given in ref [3]. The NP effects are encoded in the NP WCs C_i, C'_i and C''_i . Each primed and double primed operator can be expressed as a linear combination of unprimed operators through Feirz transformation.

The values of NP WCs which fit the data on the observables R_D , R_{D^*} , $R_{J/\psi}$, $P_\tau(D^*)$ and $\mathcal{B}(B_c \rightarrow \tau\bar{\nu})$, have been calculated previously [2]. Here $R_{J/\psi}$ is the ratio of $\mathcal{B}(B_c \rightarrow J/\psi\tau\bar{\nu})$ to $\mathcal{B}(B_c \rightarrow J/\psi\mu\bar{\nu})$ [6]. The results of these fits are listed in table 1. This table also lists, for each of the NP solutions, the predicted values of the polarization fractions and the angular asymmetries in $B \rightarrow D^*\tau\bar{\nu}$ decay. Here we compute $A_{FB}(q^2)$ and $A_{LT}(q^2)$ in $B \rightarrow D^*\tau\bar{\nu}$ decay, as functions of $q^2 = (p_B - p_{D^*})^2$, where p_B and p_{D^*} are the four momenta of B and D^* respectively. The predictions

NP WCs	Fit values	$\langle P_\tau(D^*) \rangle$	$\langle f_L \rangle$	$\langle A_{FB} \rangle$	$\langle A_{LT} \rangle$
SM	$C_i = 0$	-0.499 ± 0.004	0.45 ± 0.04	-0.011 ± 0.007	-0.245 ± 0.003
C_{V_L}	0.149 ± 0.032	-0.499 ± 0.004	0.45 ± 0.04	-0.011 ± 0.007	-0.245 ± 0.003
C_T	0.516 ± 0.015	$+0.115 \pm 0.013$	0.14 ± 0.03	-0.114 ± 0.009	$+0.110 \pm 0.009$
C_{S_L}''	-0.526 ± 0.102	-0.485 ± 0.003	0.46 ± 0.04	-0.087 ± 0.011	-0.211 ± 0.008
(C_{V_L}, C_{V_R})	$(-1.286, 1.512)$	-0.499 ± 0.004	0.45 ± 0.04	-0.371 ± 0.004	$+0.007 \pm 0.004$
(C_{V_L}', C_{V_R}')	$(0.124, -0.058)$	-0.484 ± 0.005	0.45 ± 0.04	-0.003 ± 0.007	-0.243 ± 0.003
(C_{S_L}'', C_{S_R}'')	$(-0.643, -0.076)$	-0.477 ± 0.003	0.46 ± 0.04	-0.104 ± 0.005	-0.202 ± 0.002

Table 1 Best fit values of NP WCs at $\Lambda = 1$ TeV, taken from table IV of ref. [2]. We provide the predictions of $\langle P_\tau(D^*) \rangle$, $\langle f_L \rangle$, $\langle A_{FB} \rangle$ and $\langle A_{LT} \rangle$ in decay $B \rightarrow D^* \tau \bar{\nu}$ with their uncertainties for each of the allowed solutions.

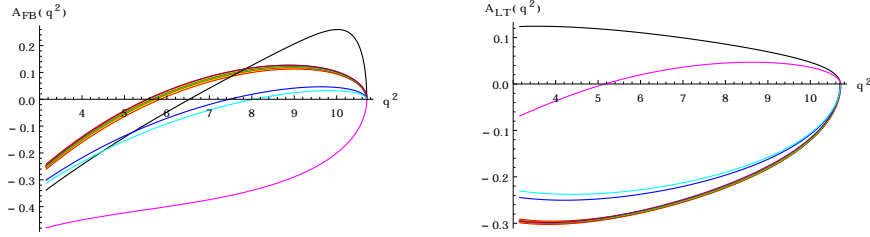


Fig. 1 Left and right panels correspond to $A_{FB}(q^2)$ and $A_{LT}(q^2)$, respectively for the $B \rightarrow D^* \tau \bar{\nu}$ decay. Red curves with yellow band corresponds to SM predictions. The band, representing 1σ range, is mainly due to the uncertainties in various hadronic form factors and is obtained by adding these errors in quadrature. In each panel, the color code for the NP solutions is: $C_{V_L} = 0.149$ (green curve), $C_T = 0.516$ (black curve), $C_{S_L}'' = -0.526$ (blue curve), $(C_{V_L}, C_{V_R}) = (-1.286, 1.512)$ (magenta curve), $(C_{V_L}', C_{V_R}') = (0.124, -0.058)$ (purple curve), $(C_{S_L}'', C_{S_R}'') = (-0.643, -0.076)$ (cyan curve).

for $P_\tau(D^*)$, f_L and A_{FB} are calculated using the framework provided in [7] and for $A_{LT}(q^2)$ we follow ref [8, 9].

The $B \rightarrow D^{(*)} l \bar{\nu}$ decay distributions depend upon hadronic form-factors. The form factors for $B \rightarrow D$ decay are well known in lattice QCD [10] and we use them in our analyses. For $B \rightarrow D^*$ decay, the HQET parameters are extracted using data from Belle and BaBar experiments along with lattice inputs. In this work, the numerical values of these parameters are taken from refs. [11] and [1].

This table lists six different NP solutions but only the first four solutions are distinct [2]. Thus we have four different NP solutions with different Lorentz structures. We explore methods to distinguish between them.

3 Results and Discussions

The average values of $P_\tau(D^*)$ and f_L for all six NP solutions are given in table 1. Not surprisingly, there is a large difference between the predicted values for O_T solution and those for other NP solutions. If either of these observables is measured with an

absolute uncertainty of 0.1, then the O_T solution is either confirmed or ruled out at 3σ level.

We now show that the angular asymmetries A_{FB} and A_{LT} have a good discrimination capability between the three remaining NP WCs. The plots for A_{FB} and A_{LT} as a function of q^2 are shown in the bottom row of fig. 1 and their average values are listed in table 1. We see that the plots of both $A_{FB}(q^2)$ and $A_{LT}(q^2)$, for (O_{V_L}, O_{V_R}) solution, differ significantly from the plots of all other NP solutions as do the average values. If either of these asymmetries is measured with an absolute uncertainty of 0.07, then the (O_{V_L}, O_{V_R}) solution is either confirmed or ruled out at 3σ level.

So far we have identified observables which can clearly identify the O_T and the (O_{V_L}, O_{V_R}) solutions. As we can see from table 1, one needs to measure $\langle A_{FB} \rangle$ with an absolute uncertainty of 0.03 or better to obtain a 3σ distinction between O_{V_L} and O'_{S_L} solutions. However, this ability to make the distinction can be improved by observing q^2 dependence of A_{FB} for these solutions. We note that $A_{FB}(q^2)$ for O_{V_L} solution has a zero crossing at $q^2 = 5.6 \text{ GeV}^2$ whereas this crossing point occurs at $q^2 = 7.5 \text{ GeV}^2$ for O'_{S_L} solution. A calculation of $\langle A_{FB} \rangle$ in the limited range $6 \text{ GeV}^2 < q^2 < q^2_{max}$ gives the result +0.1 for O_{V_L} and +0.01 for O'_{S_L} . Hence, determining the sign of $\langle A_{FB} \rangle$, for the full q^2 range and for the limited higher q^2 range, provides a very useful tool for discrimination between these two solutions.

Hence, we find that a clear distinction can be made between the four different NP solutions to the R_D/R_{D^*} puzzle by means of polarization fractions and angular asymmetries. Note that only the observables $(P_\tau(D^*))$ and f_L isolating O_T do not require the reconstruction of τ momentum. The reconstruction of τ momentum is crucial to measure the asymmetries which can distinguish between the other three NP solutions.

References

1. Y. Amhis *et al.* [HFLAV Collaboration], Eur. Phys. J. C **77** (2017) no.12, 895
2. A. K. Alok, D. Kumar, J. Kumar, S. Kumbhakar and S. U. Sankar, JHEP 09 (2018) 152
3. M. Freytsis, Z. Ligeti and J. T. Ruderman, Phys. Rev. D **92**, no. 5, 054018 (2015)
4. A. K. Alok, D. Kumar, S. Kumbhakar and S. U. Sankar, Phys. Rev. D **95**, no. 11, 115038 (2017)
5. A. K. Alok, D. Kumar, S. Kumbhakar and S. Uma Sankar, Phys. Lett. B **784** (2018) 16
6. R. Aaij *et al.* [LHCb Collaboration], Phys. Rev. Lett. **120** (2018) no.12, 121801
7. Y. Sakaki, M. Tanaka, A. Tayduganov and R. Watanabe, Phys. Rev. D **88**, no. 9, 094012 (2013)
8. A. K. Alok, A. Datta, A. Dighe, M. Duraisamy, D. Ghosh and D. London, JHEP **1111** (2011) 121.
9. M. Duraisamy, P. Sharma and A. Datta, Phys. Rev. D **90** (2014) no.7, 074013
10. S. Aoki *et al.*, Eur. Phys. J. C **77** (2017) no.2, 112
11. J. A. Bailey *et al.* [Fermilab Lattice and MILC Collaborations], Phys. Rev. D **89**, no. 11, 114504 (2014)